Proc. Natl. Acad. Sci. USA
Vol. 91, pp. 8482–8486, August 1994
Neurobiology

Striate cortex extracts higher-order spatial correlations from visual textures

KEITH P. PURPURA, JONATHAN D. VICTOR, AND EPHRAIM KATZ

Department of Neurology and Neuroscience, Cornell University Medical College, 1300 York Avenue, New York, NY 10021

Communicated by Floyd Ratliff, April 11, 1994

ABSTRACT **Spatial correlations define the statistical structure of any visual image. Two-point correlations inform the visual system about the spatial frequency content of an image. Higher-order correlations can capture salient features such as object contours. We studied "isodipole" texture discrimination in V1 to determine if higher-order spatial correlations can be extracted by early stages of cortical processing. We made epicortical, local field potential, and single-cell recordings of responses elicited by isodipole texture interchange in anesthetized monkeys. Our studies demonstrate that single neurons in V1 can signal the presence of higher-order spatial correlations in visual textures. This places a computational mechanism, which may be essential for form vision at the earliest stage of cortical processing.**

How are salient features extracted given the huge amount of information available in a visual image? It has been shown that the retina performs a crucial initial stage of information reduction through the mechanisms of light adaptation, center-surround antagonism, and spatial filtering (1–3). These mechanisms utilize the first- and second-order statistics (mean light level and spatial contrast) in the retinal image. The residual redundancy (information content) remaining in the retinal output, arising from higher-order correlations in the visual scene, may be utilized by the visual cortex to perform the necessary information reduction required for the perception and recognition of objects. The cortex may accomplish redundancy detection by linking the locally filtered regions provided by retinal processing into extended contours. Images whose redundancy is manifest by higher-order correlations in appropriate spatial configurations would invoke the linking mechanism, whereas others, with a lesser or different type of redundancy, would not. In this way, the linking mechanism could signal the presence of an object such as a fruit in the variegated canopy of a tree. It would also be more efficient for processing in extrastriate cortex if V1 reduced the number of variables (neural signals) required for representing object contours or surface borders.

To date, most single-unit studies in V1 have sought to demonstrate and model the spatiotemporal filtering properties of receptive fields. The overwhelming success of these efforts has led to the view that V1 functions as a bank of linear spatiotemporal filters, alone or in conjunction with simple nonlinearities such as rectification (4, 30). The role these receptive field mechanisms might play in vision is still being debated. But it seems apparent, given the growing catalogue of deviations of single-cell behavior from ideal spatial Fourier analysis (5, 6), that V1 does not merely construct neural representations of the global amplitude and phase spectra of retinal images.

On the other hand, arrays of mechanisms sharing some of the most commonly recognized properties of cortical cells (spatial localization and restricted spatial frequency and orientation tuning) could efficiently encode the amplitude spectra of natural images (7). If it could be shown that amplitude spectra provided sufficient information for reconstructing visual images, then these characteristics of cortical cells might be the most important for spatial vision. Mathematically, the global amplitude spectrum is equivalent (via Fourier transformation) to the two-point correlations of intensity values. While it might appear that two-point correlations are sufficient to signal edges, this is not the case. One example of an image transformation that preserves two-point correlations is a randomization of spatial phases. Randomization of spatial phases, which necessarily preserves the Fourier amplitude spectrum, destroys visually salient features such as edges. The visual cortex must, therefore, have mechanisms capable of recovering structure within the spatial phase spectrum. This is equivalent to having mechanisms capable of detecting spatial correlations involving three or more points in the image.

Psychophysics does provide evidence that the visual system can rapidly discriminate among certain textures that differ in higher-order (third or higher) statistics but that are identical at second order—i.e., share the same spatial power spectra ("isodipole" textures) (29). Thus, the visual system must be able to make use of image statistics other than two-point correlations. Linear spatiotemporal filtering, even with the added attribute of orientation tuning, cannot be invoked to explain these findings, since linear filters cannot detect spatial correlations higher than second order. However, oriented filters, combined with a special set of nonlinearities (see below), may be a key computational component V1 uses for detecting these higher-order correlations.

The ability of the visual system to utilize higher-order image statistics has been shown through the use of a variety of isodipole textures in both human visual evoked potential (VEP) and psychophysical studies (8–11). These studies have demonstrated that only certain spatial arrangements of statistically redundant structures are visually salient. The subset that is salient suggests the following physiologically plausible model: a local nonlinear subunit that extracts spatial contrast (local edge detector) is followed by a second nonlinearity that links multiple subunits sharing a common orientation preference (11). The linking nonlinearity allows the subunits to interact cooperatively so that only coactivated arrays of subunits lead to a response. The nature of the linking mechanism, whether operating by setting thresholds in the subunits or by adjusting their contrast gain, has yet to be determined. However, as we show here, evidence for this mechanism appears in V1 for a wide range of receptive field sizes. This may allow V1 to use spatial linking to extract higher-order correlations at multiple spatial scales in the visual scene.

The publication costs of this article were defrayed in part by page charge payment. This article must therefore be hereby marked "*advertisement*" in accordance with 18 U.S.C. §1734 solely to indicate this fact.

Abbreviations: VEP, visual evoked potential; CSD, current source density.

METHODS

Fig. 1 illustrates three isodipole textures: "even," "odd," and "random." The even and odd textures are generated by simple two-dimensional recursion rules from sets of randomly chosen values for the texture's initial rows and columns. If we denote the color (black or white) of the check in the *i*th row and *j*th column of the two-dimensional check array by $a_{i,j} = +1/-1$, and the colors of checks in the initial row and column ($a_{0,j}$ and $a_{i,0}$) are randomly assigned values of +1 or −1, a recursion rule determines the assignment of the interior checks of the texture from those previously assigned. For example, the interior checks of an even texture are assigned by the rule $a_{i+1,j+1} = a_{i,j+1} \times a_{i+1,j} \times a_{i,j}$. For the odd texture, the recursion rule is $a_{i+1,j+1} = (-1) \times a_{i,j+1} \times a_{i+1,j} \times a_{i,j}$. Thus, the four vertices of any rectangle in an even texture have an even number (0, 2, or 4) of black and white checks. This is the fourth-order correlation that characterizes the even texture. In the odd texture, the vertices of every 2 × 2 square have an odd number (1 or 3) of black and white checks. No second-order or third-order correlations exist for the even or odd textures. No correlations (second order or of any higher order) exist for the random textures.

Each permutation of colorings of the initial row and column generates a new even or odd texture. The collection of all possible configurations of the texture is known as the texture ensemble. As in all discussions concerning the statistical properties of textures, the power spectra of a texture only make sense in the context of repeated sampling from the texture ensemble. Thus, even, odd, and random textures are isodipole in the sense that their respective ensembles share the same power spectra.

Textures with higher-order spatial correlations have greater redundancy (less information content) than random textures. The information content of a sample of a random texture is proportional to the number of checks it contains, whereas the information content of a sample of even or odd texture is proportional to the number of checks in its first row and first column. Thus, for a 64 × 64 element texture sample, the random sample has ≈32 times the information content of the even texture sample. Again, the information content of a texture sample only makes sense in the context of repeated sampling from the texture ensemble.

Repeated interchange between different members of the even and random ensembles presents the visual system with the same spatial frequency input (two-point correlation), *on average*, across the cycle of interchange. Mechanisms sensitive only to the local or global spatial frequency content or luminance of the stimuli will, *on average*, produce the same response to the presentation of the even textures as they do to the random textures and produce a response that is "symmetric" across the cycle of interchange. Mechanisms sensitive to what differs between the two ensembles (spatial correlations of 4th- or higher-order) will, *on average*, produce a different response to each half-cycle of stimulation; the response is "antisymmetric" across the interchange cycle. Thus, the antisymmetric component of the response averaged over many cycles of even/random, even/odd, or odd/random interchange reveals mechanisms sensitive to higher-order spatial correlations. Psychophysical and VEP studies (8–11), as well as the present study, include a control for the deviation of the statistics of individual examples from those of the ensemble (i.e., random/random interchange).

Simulations (9) have demonstrated that a receptive field modeled as a linear spatial filter followed by rectification will fail to produce a large antisymmetric response component that survives averaging over multiple presentations of isodipole texture interchange. Y cells in the lateral geniculate nucleus of the cat, which can be modeled with a one-stage nonlinearity (12), show minimal antisymmetric responses to even/odd texture interchange (2.1% of the total power in the odd harmonics of the response of single Y cells and 0.3% for this component in multiunit Y-cell recordings) (13). Our previous work (8–11) indicates that two stages of nonlinearity, as described above, are required to account for the selective presence of large antisymmetric responses (≈25% of the total power contained in odd harmonics) to certain textures differing in third- and higher-order statistics.

RESULTS

Fig. 2 shows that there are mechanisms in the monkey visual cortex that can discriminate between textures differing in certain fourth-order spatial correlations. A prominent antisymmetric VEP component is generated by even/random and even/odd interchange, interchanges where there is repeated modulation of fourth- and higher-order spatial correlations. In the random/random interchange, the statistics of the textures do not change across the averaging cycle so no antisymmetric component is generated; the symmetric response, not shown here, is the same as the raw VEP.

The results shown in Fig. 2 suggested that mechanisms sensitive to fourth-order spatial correlations could be found in V1. To verify that neural populations in striate cortex do generate signals consistent with those seen in Fig. 2, we made intracortical field potential recordings within monkey V1.

Intracortical field potentials were sampled simultaneously from different depths within parafoveal V1 with a 16-element electrode (15) and submitted to current source density (CSD) analysis (16). Results similar to those shown in Fig. 3 were obtained from all electrode placement sites in V1. Antisymmetric current responses were produced by interchanging textures differing in higher-order spatial correlations (even/random, even/odd, and odd/random interchange). The control condition (random/random interchange) produced no antisymmetric components. This is a key control because it indicates that differences between texture examples drawn from the same ensemble do not produce an antisymmetric response component. The fact that even/random interchange produces larger antisymmetric components than even/odd

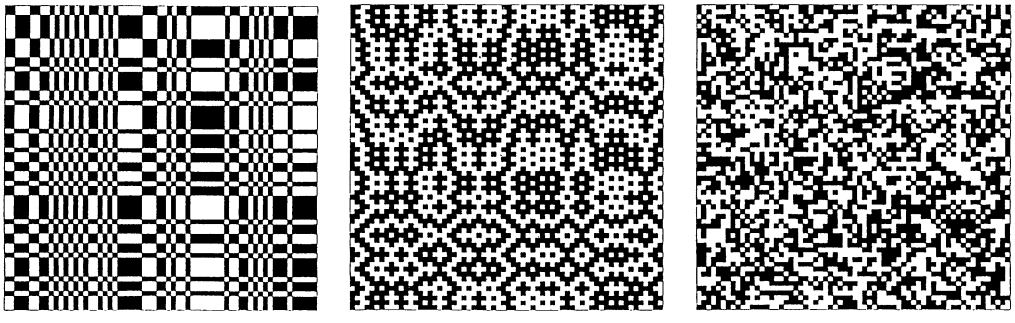

FIG. 1. Isodipole textures. Samples drawn from even (*Left*), odd (*Center*), and random (*Right*) isodipole texture ensembles.

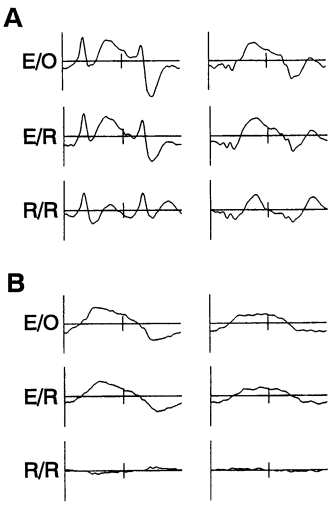

FIG. 2. Monkey VEPs elicited by isodipole texture interchange. Achromatic isodipole textures were presented to 15 anesthetized and paralyzed cynomolgus monkeys (*Macaca fascicularis*) using standard techniques for surgical preparation and maintenance of vegetative physiology (14). In 10 of the experiments, urethane (20 mg per kg per hr with a maximum dose of 1 g) was used as the general anesthetic, and in the others sufentanil citrate (6 μg per kg per hr) was employed. Similar results were obtained with the two anesthetics. In this figure, the waveforms are averaged from 128 cycles of texture interchange; each cycle of the interchange lasted 473 msec. Different samples of even and random textures were presented for each cycle. Results are shown for even/odd (E/O), even/random (E/R), and random/random (R/R) interchange. The interchange occurred at the time marked by the vertical line in the time base of the recordings. Random/random interchange serves as an important control because local luminance and spatial frequencies are the same as they are for the even/random and even/odd conditions. Shown in *A* are the raw VEP signals, and in *B* the antisymmetric components (odd harmonics) extracted from the raw signals are presented. The waveforms in *Left* (both *A* and *B*) were recorded differentially from a screw placed above the right opercular cortex. The waveforms in *Right* (both *A* and *B*) were recorded from an electrode placed directly on the pia of the left striate cortex. Screw and pial recordings were made concurrently (0.03–100 Hz, 10,000 gain). Vertical bars indicate 75 μV. Visual stimulation was binocular and unit check size was 27′ of arc. The textures subtended 14° × 14° of visual angle. Luminance contrast was 100%. Not shown here or in Figs. 3 and 4 are studies made parametric in contrast. In general, antisymmetric responses increased in amplitude with increasing luminance contrast.

interchange implies that a mechanism, such as rectification or summation of the output of a number of rectifying subunits, cannot account for these results (9, 10). The distribution of antisymmetric components throughout the cortical layers and the multiple inversions of polarity suggest that no one subpopulation of cortical cells or cortical laminae in V1 produces the texture interchange signals. Thus, mechanisms sensitive to higher-order spatial correlations appear to be distributed throughout the depth of parafoveal V1.

The size and laminar distribution of the antisymmetric currents elicited by isodipole texture interchange suggest that many neurons in V1 are involved in extracting higher-order spatial correlations from textures. To determine if all neurons have this property, single-unit recordings were made in monkey V1.

Twenty single-unit recordings were made in parafoveal V1 of five monkeys. The size of the building block checks in these studies was 2.8′ × 2.8′ of arc for all textures. The receptive fields of the neurons studied here ranged in area from 0.1 deg^2 to 2.2 deg^2. The number of texture elements captured by the smallest receptive fields was, therefore, between 30 and 40, whereas the largest receptive fields could enclose nearly 800 of the smallest texture elements. The small size of the texture elements, in combination with the presentation of many samples from the texture ensemble during the stimulation period, allowed the restricted receptive fields of the parafoveal units to vignette enough of the texture to obtain an accurate estimate of the texture's statistics.

Six of the cells were classified as simple cells, five were classified as complex, and nine were not classified. Of the four simple cells that responded to isodipole texture interchange, two had antisymmetric response components, and two had only symmetric responses. All of the other cells (two of the complex cells and five of the unclassified cells) that responded to texture interchange also had antisymmetric responses.

Fig. 4 shows recordings from three single units recorded in V1. The two simple cells in Fig. 4 both show a significant suppression of firing during the presentation of the even textures in the even/random interchange. This coincides with an antisymmetric component in the simultaneously recorded local field potential. The complex cell, on the other hand, shows an enhancement of firing during the presentation of the even textures. The other complex cell that responded to isodipole texture interchange had the same response properties as those shown in Fig. 4*C*. Note that the control condition (random/random interchange) elicited very little differential response to texture interchange. Thus, single units in V1, both simple and complex, can signal the presence of higher-order spatial correlations in visual textures. Not shown in Fig. 4*C* is that the complex cell could also readily discriminate between odd and random textures.

The prominent symmetric responses in Fig. 4 *A* and *B* are probably due to simpler nonlinearities like rectification and saturation. The sensitivity of simple cells to spatial phase cannot account for the results in Fig. 4 *A* and *B* because the ensemble of isodipole textures assures that the phases of constituent spatial harmonics are randomized over the averaging period. A neuron must be sensitive to a set of relative spatial phases in order to be able to discriminate between textures differing in fourth-order correlations. This requires a cortical receptive field nonlinearity that has not been previously described. Note that the texture elements used in the monkey VEP and CSD depth-profile studies are 125 times larger in area than those used in the single-unit studies. These texture elements would cover all but the largest receptive fields in V1 in their entirety. Thus, the antisymmetric responses shown in Fig. 3 probably arise from neurons recruited from the subpopulation in V1 with the largest receptive fields. Alternatively, these responses could represent some emergent property of the local cortical network, which is reflected in the population response inherent in the VEP and CSD data. The fact that not all single-cell recordings displayed sensitivity to higher-order spatial correlations suggests that there is some division within the V1 population with respect to this property. However, the segregation does not coincide with the conventional simple/complex cell dichotomy.

The ensemble properties of isodipole textures constrain the types of receptive field mechanisms that can produce antisymmetric responses to texture interchange, even for receptive fields that sample very restricted portions of the textures. For example, if a receptive field is so small that it is covered by only a single texture element, there are four equally likely transitions of luminance in the receptive field at the time of texture interchange: dark to dark, light to light, light to dark, and dark to light. All of these occur with equal probability at both transitions of the stimulus cycle (even/random and random/even) so all occur with the same frequency over the stimulation period. Thus, regardless of the nature of the nonlinearity conjoined with the receptive field, no net antisymmetric response can survive the ensemble averaging, and only a symmetric component could be generated. A similar argument holds for a neuron that receives input from only two or three checks; there are 16 or 64 equally likely transitions,

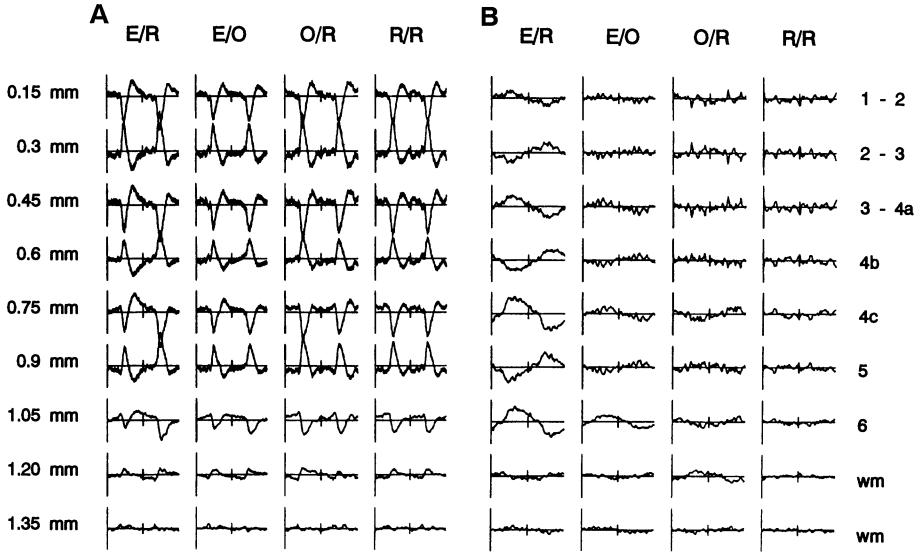

FIG. 3. Intracortical responses to texture interchange recorded in monkey V1. Multielement electrode recordings were made at 13 electrode placement sites in six animals. The position of the electrode with respect to the V1/V2 border and orientation with respect to the cortical laminae were determined by histological recovery of a lesion produced at one of the electrode's elements (5 μA for 5 sec). Alternate sections of cortical tissue were stained for cytochrome oxidase (17) and with Nissl. Interelement distance on the electrode was 150 μm. Vertical movement of the electrode demonstrated that the observed variation in response amplitude with cortical depth was not a consequence of differences in resistivity of the recording elements. Gain and bandwidth for the local field potential recordings were the same as in Fig. 2. Shown here are responses recorded at one electrode placement site. The period of interchange was 473 msec. Each column was the result of averaging over 384 cycles of interchange. Unit check size of the textures was 27′ × 27′ of arc. Textures had a luminance contrast of 100% and subtended 14° × 14° of angle. Stimulation was monocular. The numbers at the left indicate the depth of the recording element with respect to the cortical surface. The numbers at the right indicate the estimated positions in the cortical laminae of the recording elements. A designation of "1-2" is meant to convey that the recording element straddled the border of laminae 1 and 2. wm, White matter. (*A*) Raw current signal extracted from the local field potentials recorded from 9 of the 15 electrode elements. The values are proportional to the CSD and were obtained by subtracting differentially recorded signals at adjacent pairs of electrodes. The constant of proportionality depends on the conductivity of the cortical tissue, a property that was not measured here. Vertical scale = 2000 μV/mm^2. (*B*) Antisymmetric component of the current signals. Vertical scale = 1000 μV/mm^2. E/O, even/odd interchange; E/R, even/random interchange; O/R, odd/random interchange; R/R, random/random interchange.

respectively, possible through each interchange. The antisymmetric responses reported here must involve receptive field mechanisms that receive input from at least four texture elements. It is at this level of spatial sampling that the fourth-order correlations in the even textures begin to generate an imbalance in the distribution of possible configurations of dark and light elements in the receptive field during even/random interchange. For these larger receptive fields, more detailed arguments and calculations (9, 10) show that a single stage of rectification cannot account for the antisymmetric responses.

DISCUSSION

Mechanisms that integrate local elements in a visual scene are often assumed to be situated in the extrastriate cortex. Recent studies, however, indicate that such spatial integra-

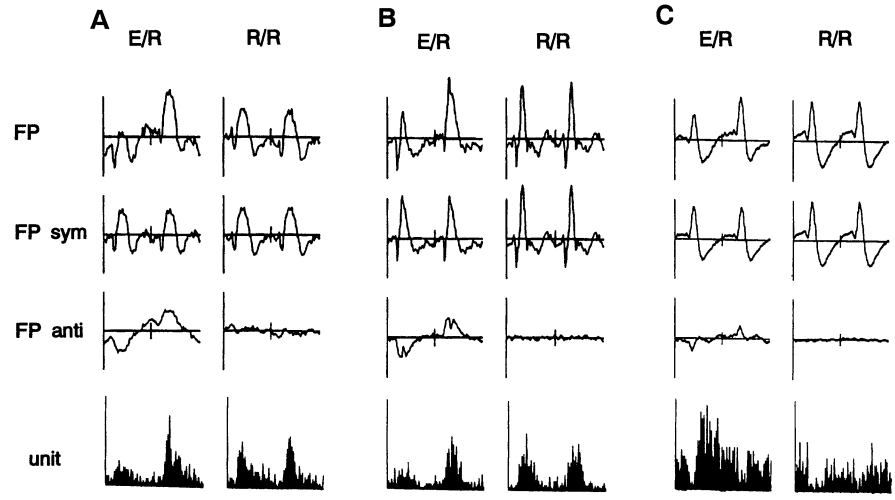

FIG. 4. Responses of single units to isodipole texture interchange. Cells were mapped and classified with hand-held stimuli and gratings displayed on a cathode ray tube. Data are presented from two simple cells (*A* and *B*) and one complex cell (*C*). All cells were within 5° eccentricity of the fovea. Local field potentials and spike activity were recorded off the same Ainsworth tungsten-in-glass microelectrode. Local field potentials were obtained by low-pass filtering the microelectrode signal with a bandwidth of 0.03–60 Hz and a 6 dB per octave roll-off. Luminance contrast of the textures was 100%. (*A*) Simple cell. Vertical scale (Vs) local field potential (FP), 40 μV. Vs unit, 40 impulses per sec (ips). (*B*) Simple cell. Vs FP, 20 μV; Vs unit, 40 ips. (*C*) Complex cell. Vs FP, 70 μV; Vs unit, 20 ips. E/R, even/random interchange; R/R, random/random interchange.

tion is not restricted to regions outside V1. Extraction of contour from motion and texture segregation based on local feature orientation have been shown in monkey V1 (18–20) at the level of neural populations. Single-unit studies in monkey V1 (21) and cat A17 (6) suggest that orientation interactions between the classical receptive field and far-field surround may underlie these operations. Illusory contours, once thought to be encoded first in the cortical processing stream by neurons in V2 (22), have also now been shown to drive single neurons in V1 (23). Our finding, that V1 extracts higher-order spatial correlations, provides a third line of evidence that V1 is engaged in the processing of visual form. Because the statistical structure of isodipole textures is scale independent, we were also able to show here that a spatial linking operation occurs in V1 at multiple spatial scales. This places even more emphasis on V1's role in the inferotemporal "what" pathway of the primate cortex.

Our recordings show that single neurons in V1 can extract certain higher-order spatial correlations from visual textures. Linear summation, simple spatial phase sensitivity, rectification, or energy computations cannot account for these results. A successful model requires cooperative interaction among spatial subunits—i.e., a spatial linking mechanism (11). The spatial subunits of the computational model may be realized in the monkey cortex as the subunits of certain receptive fields. Our results show that these receptive fields are not rare and have a wide range of sizes in parafoveal cortex. We conclude that V1 has an essential property required for the detection of redundancy in the retinal image: sensitivity to higher-order spatial correlations.

The limited repertoire of redundant structures that the visual system finds salient may be a consequence of a bias V1 has for special spatial features (textons) it can capture with a particular nonlinearity (spatial linking). In our studies, these textons may be the elongated oriented edges in the even textures. While it has been recognized for decades that striate neurons can be selectively activated by such local features as elongated blobs and oriented edges (24), we show here that many neurons in V1 use a nonlinear mechanism for producing this selectivity and that this response property is useful for texture discrimination. Our work, as well as that of those mentioned above (6, 18–21, 23), suggests that the entire computational repertoire of single neurons in V1 has yet to be fully documented. Bringing these capacities to light will require a willingness to employ unconventional stimuli, as we do here.

Our reliance on stimuli whose salient features are manifest in global as well as local statistics is not at odds with the view (25, 26) that texture discrimination is driven by local processing. It is precisely because the extraction of features is nonlinear that such local signals survive spatial or ensemble averaging and are detected by our experimental technique.

Demonstration of sensitivity of V1 to higher-order correlations does not imply that a statistical order-by-order approach is the optimal description of images or of visual processing. Rather, it emphasizes the need to develop a solid theoretical foundation for the structure of natural images that supersedes linear spatial filtering (27, 28) by recognizing the role of the nonlinear processing of local features and to apply such ideas to neurophysiology.

K.P.P. was supported by the McDonnell–Pew Program in Cognitive Neuroscience and the Revson Foundation. J.D.V. was supported by National Institutes of Health Grant EY9314. E.K. was supported by the Revson Foundation.

1. Srinivasan, M. V., Laughlin, S. B. & Dubs, A. (1982) *Proc. R. Soc. London B* **216,** 427–459.
2. Shapley, R. M. & Enroth-Cugell, C. (1984) *Prog. Retinal Res.* **3,** 263–346.
3. Laughlin, S. B. (1989) *J. Exp. Biol.* **146,** 39–62.
4. Landy, M. S. & Movshon, J. A. (1991) *Computational Models of Visual Processing* (MIT Press, Cambridge, MA), p. 394.
5. Shapley, R. & Lennie, P. (1985) *Annu. Rev. Neurosci.* **8,** 547–583.
6. Bonds, A. B. (1989) *Visual Neurosci.* **2,** 41–55.
7. Field, D. J. (1987) *J. Opt. Soc. Am.* **A4,** 2379–2394.
8. Victor, J. D. & Zemon, V. (1985) *Vision Res.* **25,** 1829–1844.
9. Victor, J. D. (1985) *Vision Res.* **25,** 1811–1827.
10. Victor, J. D. & Conte, M. M. (1989) *Visual Neurosci.* **2,** 297–313.
11. Victor, J. D. & Conte, M. M. (1991) *Vision Res.* **31,** 1467–1488.
12. Hochstein, S. & Shapley, R. M. (1976) *J. Physiol. (London)* **262,** 237–264.
13. Victor, J. D. (1986) *Proc. Natl. Acad. Sci. USA* **83,** 7984–7988.
14. Purpura, K., Tranchina, D., Kaplan, E. & Shapley, R. M. (1990) *Visual Neurosci.* **4,** 75–93.
15. Schroeder, C. E., Tenke, C. E., Arezzo, J. C. & Vaughan, H. G., Jr. (1988) *Invest. Ophthalmol. Visual Sci.* **29,** Suppl., 329.
16. Freeman, J. A. & Nicholson, C. (1975) *J. Neurophysiol.* **38,** 369–382.
17. Hevner, R. F. & Wong-Riley, M. T. T. (1990) *J. Neurosci.* **10,** 1331–1340.
18. Lamme, V. A. F., Van Dijk, B. W. & Spekreijse, H. (1992) *Vision Res.* **32,** 797–807.
19. Lamme, V. A. F., Van Dijk, B. W. & Spekreijse, H. (1993) *Nature (London)* **363,** 541–543.
20. Lamme, V. A. F., Van Dijk, B. W. & Spekreijse, H. (1993) *Visual Neurosci.* **10,** 781–790.
21. Knierim, J. J. & Van Essen, D. C. (1992) *J. Neurophysiol.* **67,** 961–980.
22. von der Heydt, R., Peterhans, E. & Baumgartner, G. (1984) *Science* **224,** 1260–1262.
23. Grosof, D. H., Shapley, R. M. & Hawken, M. J. (1993) *Nature (London)* **365,** 550–552.
24. Hubel, D. H. & Wiesel, T. N. (1968) *J. Physiol. (London)* **195,** 215–243.
25. Julesz, B. (1991) *Rev. Mod. Phys.* **63,** 735–772.
26. Kovacs, I. & Julesz, B. (1993) *Proc. Natl. Acad. Sci. USA* **90,** 7495–7497.
27. Atick, J. J. (1992) *Network* **3,** 213–251.
28. Knill, D. C., Field, D. & Kersten, D. (1990) *J. Opt. Soc. Am.* **A7,** 1113–1123.
29. Julesz, B., Gilbert, E. N. & Victor, J. D. (1978) *Biol. Cyb.* **31,** 137–149.
30. Zhou, Y. & Baker, C. L. (1993) *Science* **261,** 98–101.